Nuclear Engineering and Technology 54 (2022) 4671–4678

Contents lists available at ScienceDirect

Nuclear Engineering and Technology

journal homepage: www.elsevier.com/locate/net

Original Article

Towards a better understanding of detection properties of different types of plastic scintillator crystals using physical detector and MCNPX code

Ayberk Yilmaz [a, *], Hatice Yilmaz Alan [b], Lidya Amon Susam [a], Baki Akkus [a, **], Ghada ALMisned [c], Taha Batuhan Ilhan [d], H.O. Tekin [e, f]

[a] Department of Physics, Faculty of Science, Istanbul University, 34134, Istanbul, Turkey
[b] Institute of Nuclear Sciences, Ankara University, 06100, Ankara, Turkey
[c] Department of Physics, College of Science, Princess Nourah Bint Abdulrahman University, P.O. Box 84428, Riyadh, 11671, Saudi Arabia
[d] Yildiz Technical University, Faculty of Electrical and Electronics, Control and Automation Engineering Department, Istanbul, Turkey
[e] Department of Medical Diagnostic Imaging, College of Health Sciences, University of Sharjah, 27272, Sharjah, United Arab Emirates
[f] Istinye University, Faculty of Engineering and Natural Sciences, Computer Engineering Department, Istanbul, 34396, Turkey

ARTICLE INFO

Article history:
Received 24 April 2022
Received in revised form
4 July 2022
Accepted 31 July 2022
Available online 27 August 2022

Keywords:
MCNP
Plastic scintillator
Radiation
Polystrene
Detector

ABSTRACT

The purpose of this comprehensive research is to observe the impact of scintillator crystal type on entire detection process. For this aim, MCNPX (version 2.6.0) is used for designing of a physical plastic scintillation detector available in our laboratory. The modelled detector structure is validated using previous studies in the literature. Next, different types of plastic scintillation crystals were assessed in the same geometry. Several fundamental detector properties are determined for six different plastic scintillation crystals. Additionally, the deposited energy quantities were computed using the MCNPX code. Although six scintillation crystals have comparable compositions, the findings clearly indicate that the crystal composed of PVT 80% + PPO 20% has superior counting and detecting characteristics when compared to the other crystals investigated. Moreover, it is observed that the highest deposited energy amount, which is a result of the highest collision number in the crystal volume, corresponds to a PVT 80% + PPO 20% crystal. Despite the fact that plastic detector crystals have similar chemical structures, this study found that performing advanced Monte Carlo simulations on the detection discrepancies within the structures can aid in the development of the most effective spectroscopy procedures by ensuring maximum efficiency prior to and during use.

1. Introduction

When exposed to ionizing radiation, scintillators release photons. In 1895, BaPt(CN)4 was characterized as the first scintillator for X-ray detection [1]. Scintillation detectors are frequently employed in high energy physics and nuclear physics for radiation and particle detection as well as industrial measurement. Scintillators made of plastic (polymer) are utilized in a variety of radiation monitoring applications. Recent years have seen a rise in interest in the development of high-efficiency plastic detectors. This type of detectors offers a number of benefits, including rapid rise and decay rates, excellent optical transmission, cheap cost, large useable size, high optical uniformity, mechanical stability, and ease of dopant addition. Plastic scintillation detectors are available in a variety of shapes and sizes. Plastic scintillators are manufactured by immersing the scintillator in a suitable base and then polymerizing the mixture. Typically, the combination is composed of polystyrene (PS), polymethylmethacrylate (PMMA), or polyvinyltoluene (PVT) monomer [2]. The plastic scintillator transforms the energy emitted by ionizing radiation into light pulses. Schorr and Torne developed the plastic scintillator in 1950 [3,4]. This first plastic was created by dissolving m-terphenyl in polystyrene. Numerous formulations have been developed to improve scintillation efficiency. Plastic scintillators are a more cost-effective option since they are based on low-cost commodity polymers such as poly (vinyl toluene) (PVT) or

* Corresponding author.
** Corresponding author.
E-mail addresses: ayberk@istanbul.edu.tr (A. Yilmaz), akkus@istanbul.edu.tr (B. Akkus).

https://doi.org/10.1016/j.net.2022.07.032

polystyrene doped with fluorescent molecules. Numerous materials may be included into plastics to improve the efficacy of the plastic scintillator detector. Plastics have been thoroughly examined in order to determine the optimal composition in terms of scintillation effectiveness, decay duration, and chemical stability, among other characteristics. Typically, plastic scintillators are made by thermal polymerization, doping, or coating with fluorescent dye [5]. Because the polymer constitutes 70–97% of the scintillator's composition, most of the energy emitted by impinging ionizing radiation is deposited here [1]. Although polystyrene serves as the main scintillator in the detector, it requires the addition of a secondary and another dopant (wavelength-shifter) due to polystyrene's significant self-absorption at its own emission wavelength (300–350 nm) [6]. Kang et al., developed a plastic scintillator for the detection of radioactive strontium and utilized Monte Carlo N-Particle (MCNP) simulation to optimize the thickness of the plastic scintillator for effective strontium detection [7]. An investigation was undertaken for the characterization of quantum dots (CdSe/ZnS) and PPO (2, 5-diphenyloxazole) doped styrene-based plastic scintillators [8]. Sujung et al. developed an integrated and portable probe based on a functioning plastic scintillator for radioactive cesium detection in 2021 [5]. Jong Soo Nam et al. evaluated the efficiency of a Plastic Scintillator for in situ Beta Measurement System [9] using the Monte Carlo radiation-transport algorithm MCNP6. Cheol and et al. published another work on the characteristics of plastic scintillators in 2016 [10]. Yuki and his colleagues conducted research to improve the detection effectiveness of plastic scintillators by introducing zirconia nanoparticles up to 30% by weight [11]. Another study investigated the properties of plastic scintillators using MCNP5 and LightTools simulations for the Electronic Personal Dosimeter application [12]. Z, Yasin, et al. [13] investigated Monte Carlo simulations and observations for determining the efficiency of lead shielded plastic scintillator detectors in 2017. The behaviour and response of a highly sensitive silver-activation detector utilized for neutron detection [14] were determined by simulations utilizing the MCNP algorithm. Rogers et al. [15] disclosed the synthesis of transparent PMMA scintillators containing 0.5 wt.% CdTe QDs. Patrick et al., reported on the production and incorporation of rationally selected organotin chemicals into polystyrene matrices as a means of developing plastic scintillators capable of gamma-ray spectroscopy [16]. Another 2011 research investigated several Efficient Dopants in Plastic Scintillators for Sensitive Nuclear Material Detection [17]. Allison and colleagues investigated the use of poly (vinyl toluene) (PVT) over doped with 2,5-diphenyloxazole and a fluorescent secondary dopant, 1,4-bis (5-phenyloxazol-2-yl) benzene, to detect and discriminate neutron and gamma radiation by scintillation [18].

Scintillators can be loaded with dopants of heavy metals or neutron absorbers so by this way the effective stopping power of any organic scintillator to gamma rays or neutrons can be improved, and this has led to larger volumes and higher scintillation light yields. An organic scintillator can be resumed as a matrix that contains one or several organic fluorophores and potentially some dopants for giving special application features, whereas these fluorophores are usually called primary and secondary fluorophores. In standard plastic scintillators, the matrix accounts for $\geq$ 95% of the material wherein the radiation/matter interaction occurs [1]. Alexander et al. studied the dose rate dependence and temporal resolution of scintillators that makes in the accurate detection of ultrahigh dose-rate (UHDR) x-rays [19]. A functional plastic scintillator was fabricated including CdTe (cadmium telluride) material for detection of radioactive cesium by Sujung et al. [20]. Experimental work on the use of MOFs (metal-organic framework) as scintillators was done by Villemot et al. and also simulated with MCNP software [21]. Alan Proctor developed a method based on Particle Swarm Optimization (PSO) which analyzes raw PVT spectra and provides a histogram of contribution vs. incident monoenergetic gamma energy and response functions for PVT were calculated using MCNP5 in this study [22]. In the study conducted by Horst et al., in 2022, multi-detector setup and simulations performed to calculate the cosmic radiation that astronauts would be exposed to [23]. Numerous optimization studies are conducted to maximize the efficiency and minimize the cost of scintillator detectors. MCNPX is a highly specialized program for improving the design and analysis of detectors. In addition, MCNPX and its optimum operating energies are lower than the Geant4 code. This is because the Geant4 code is more suitable for high energy physics applications. Considering the significant history of research on this topic and its widespread influence on the scientific literature [24–31], the purpose of this paper is to simulate the UPS-923A type plastic scintillation detector that is physically accessible in our laboratory using the MCNPX Monte Carlo code and to compare it to some other scintillation crystals proposed in previous investigations. The findings of this work may be used to advance the field of plastic scintillation detector research, which is a hot issue in the literature, as well as to get a better understanding of the probable behaviour patterns of scintillation crystals in detector structures with a certain physical form.

2. Materials and methods

2.1. Properties of modelled scintillation detector

In this study, UPS 923A, a polystyrene-based scintillator [32], was selected in terms of comparing its detection properties with some of the available plastic scintillator materials available in the literature (see Table 1). Fig. 1a shows the physical appearance of UPS-923A (50mm × 100mm × 1000mm) plastic scintillator detector. As can be seen from the figure, the detector has two components, a scintillation crystal and a PMT. The dimensions of the scintillation crystal are designed as 50mm × 100mm × 1000mm, and one end is directly connected to the PMT. Technical drawing of the UPS 923A detector taken from the user manual is shown in Fig. 1b. More detailed information about the modelled detector can be obtained from the source document available in the literature [32].

2.2. MCNPX Monte Carlo simulation studies and detector design

In this investigation, the MCNPX (Monte Carlo N-Particle eXtended) version 2.4.0 [33] was utilized to design and quantify basic detector properties of UPS 923A detector. Additionally, several kinds of plastic scintillation crystals were inserted to the scintillation crystal section of the UPS 923A detector to compare their detector responses and deposited energy amounts in the scintillation crystal. MCNPX is a fully three-dimensional (three-dimensional) general-purpose software that utilizes advanced and upgraded nuclear cross-section libraries and physics models for a variety of

Table 1
Investigated plastic scintillator detectors and crystal compositions.

Code	Plastic scintillator	Reference
bse	Polystyrene + PTP 2% + POPOP 0.03%	[**19**]
cdz	Polystyrene >99% + PPO 0.4%+POPOP 0.01%+CdS/ZnS 0.2 %	[**4**]
pp1	PVT 80% + PPO 20%	[**18**]
pp2	PVT 75% + PPO 25%	[**18**]
pp3	PVT 70% + PPO 30%	[**18**]
tz1	Polystyrene + 1.5% PTP	[**32**]

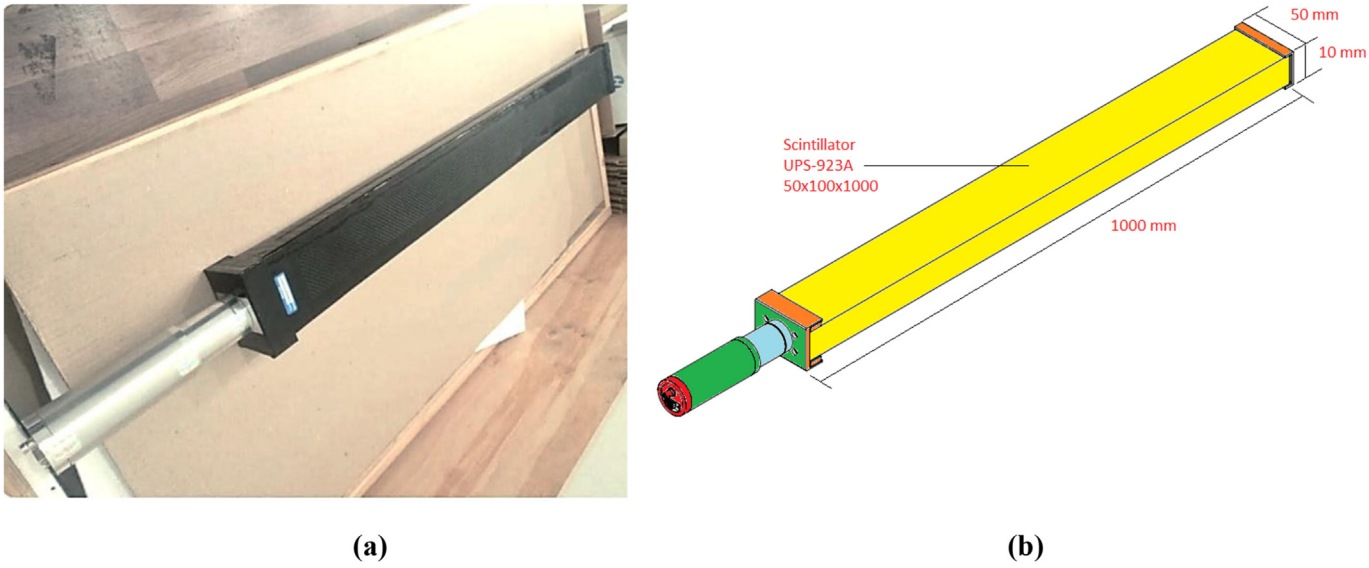

Fig. 1. (a) Physical appearance of Plastic Scintillator Detector UPS-923A 50 × 100 × 1000(b) Technical drawing taken from the user manual.

scientific applications ranging from medicine to nuclear physics [34–40]. The geometrical shape of UPS 923A detector was first modelled using the code's INPUT file as a first step in the simulation process. For this aim, a detailed INPUT file of MCNPX, which is composed of three major components such as CELL card, SURFACE card, and DATA card was successfully prepared. Initially, we determined the CELL card information of the modelled UPS 923A using surface boundaries, material definitions (wt.%) as well as tracking importance information for each cell. The exported information from the INPUT file of the defined cell number 3 of the UPS 923A plastic scintillation crystal is presented below.

3 1 -1.06 -4 5–3 2 6 -7 imp: p 1.

From the information given in this line, number 3 represents the cell number, in which the scintillation crystal is defined, the number 1 represents the material composition of the scintillation crystal defined by M1 (m1 1000–0.00700 6000 -0.92251 7000–0.00023 8000 -0.00026), and the number -1.06 represents the density (g/cm^3) of the scintillation crystal. The numbers from 3 to 7 following the density information are the code numbers of the surfaces surrounding the scintillation crystal. Each number represents a surface, and the geometric alignment of each surface with the x, y, and z axes is as follows.

2 py -5.
3 py 5.
4 pz 0.
5 pz -100.
6 px -2.5.
7 px 2.5.

Fig. 2 depicts the demonstration of modelled plastic scintillation detector obtained from MCNPX Visual Editor tool (version X22S). The UPS-923A detector's design, which is physically shown and whose technical drawing and geometrical elements are described, has been modelled in the MCNPX code and accordingly, displayed in the visualization editor. Although all the above-mentioned operations were performed for the UPS-923A detector as the first pahse, similar definitions were made separately for all plastic scintillastion crystals (see Table 1) examined in the benchmarking phase, and the essential CELL card writing actions were redefined using the elemental composition properties of each scintillation crystal. MCNPX simulations were successfully performed using an advanced Lenovo-ThinkStation® workstation with Threadripper PROHexadeca-Core (16Core) 3955WX3.90GHz-32GBDDR4SDRAM-RAM.

3. Results and discussions

3.1. Benchmarking phase for validation

The plastic scintillator's radiation simulation was performed utilizing extended version (MCNPX) of the General Monte Carlo N-Particle Transport Code. The content of the simulation was stated similarly to the real condition of UPS 923A. The 5000 cm^3 rectangular polystyrene scintillator was utilized for the test measurement. The scintillation crystal of UPS 923A detector was encoded as bse. The measurement of detector response is required for a non-isotropic radiation detector to observe the differences in a detector's behaviour based on the direction of the incoming photon. To assess the reliability and validity of the modelled detector geometry, the same parameters utilized in a previous work [4] were specified for recent detector geometry. Fig. 3 shows comparison of detector responses for MCNPX and GEANT [4] codes. A persistent trend of agreement between the spectra obtained independently of the energy areas for MCNPX and GEANT4 is noticed. However, some slight quantitative changes, notably in the low energy areas, were detected. The primary cause for this predicament might be that there are certain technical discrepancies between the codes and databases utilized. For instance, although the GEANT4 algorithm is mostly utilized for high-energy simulations, this situation is inverted in MCNP, with applications at the medical and medium energy levels.

3.2. Characterization of different plastic scintillation crystals

As a consequence of the high degree of consistency between the quantitative values acquired, we agreed to extend using the main design created in the MCNPX code and to conduct characterization activities on additional plastic scintillation crystals for the purpose of the targeted research. In the second step, different types of plastic scintillation crystals, whose elemental compositions are given in Table 1, were defined in the crystal region of the model detector shown in Fig. 2, and the MCNPX F8 tally mesh output was reported separately for each material. The F8 tally mesh provides

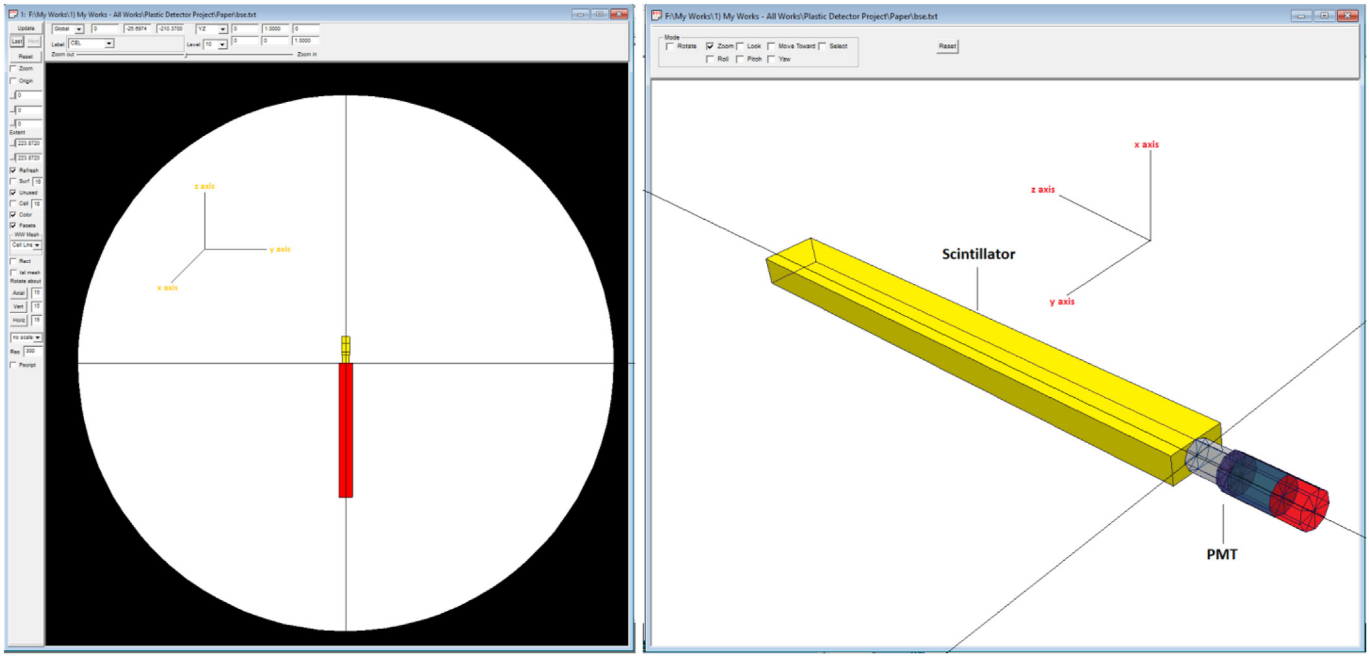

Fig. 2. Demonstration of modelled plastic scintillation detector using MCNPX Visual Editor tool (version **X22S**)(a) 2-D view **(b)** 3-D view.

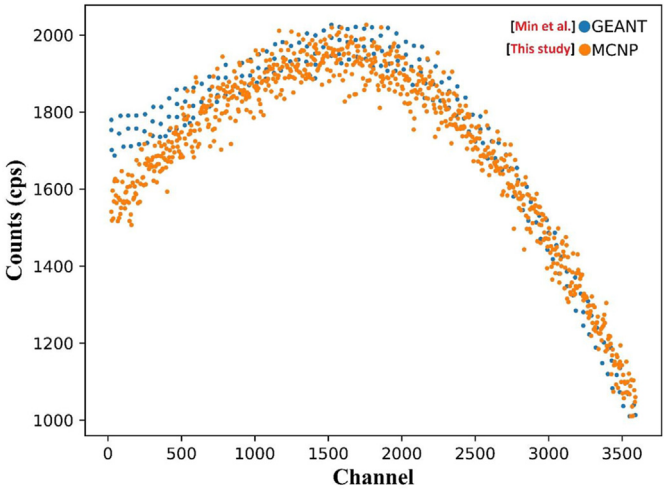

Fig. 3. Comparison of detector responses for MCNPX and GEANT [29] codes.

distribution of pulse/height within a cell. For instance, once F8 tally mesh is defined in a scintillation crystal cell, the pulse/height distribution for this crystal cell can be recorded. Fig. 4 depicts the comparison of pulse/height distributions for modelled scintillation crystals. As can be seen from the figure, the pulse/height distribution obtained from the six compared plastic scintillation crystals [4,18,27,32] exhibited similar behaviour patterns as a function of energy. However, the differences in the elemental structures of the crystals used led to some important as well as expected differences in the obtained spectrums. Although the examined plastic scintillation crystals display comparable behavioural characteristics, the bse crystal creates the smallest pulse amount (see Fig. 5) for the same energy value, while the pp1 crystal produces the largest pulse quantities. The average value of the quantitative counts acquired from the spectrums and corresponding to each energy point (8195 energy points between 0 and 2 MeV) is as follows.

i) bse - 0.000031511734834 (F8 pulse/height)
ii) cdz - 0.000031511780203 (F8 pulse/height)
iii) pp1 - 0.000031512143943 (F8 pulse/height)
iv) pp2 - 0.000031511961309 (F8 pulse/height)
v) pp3 - 0.000031511932665 (F8 pulse/height)
vi) tz1 - 0.000031512090575 (F8 pulse/height)

The numerical similarity of the obtained results may be explained by the fact that plastic detectors often have comparable chemical and elemental compositions. However, the structural alterations to the crystal are reflected in the detector's direct response functions. Similar situations have also been observed in previous studies in the literature [41,42], and chemical composition differences are reflected in the pulse/height distributions in the obtained spectra. Following the acquisition of the spectra of the modelled plastic scintillation crystals, further physical analyses of each detector were conducted. The primary motivation for doing these analyses is to gain a better understanding of the situations that result in these observed count difference values, and secondly, to gain a better understanding of other physical differences that are indirectly caused by these situations. To do this, the MCNPX OUTPUT files was thoroughly investigated, and several data on the intra-detector, crystal-gamma-ray interaction and the detection process, such as collusion per population (%) rate, average track mean free path (cm), collision weight per history were exported and examined in detail (see Table 2 and 3). Fig. 6 depicts the variation of collision per population for modelled scintillation crystals. The OUTPUT file provides information about the percentage of collisions between the particles emitting from the source and detector crystal's atomic structure. This may be seen as a measure of detection efficiency and is an essential metric since it provides information about the tendency of the particles to collide with the detector crystal. This is because each signal produced by a

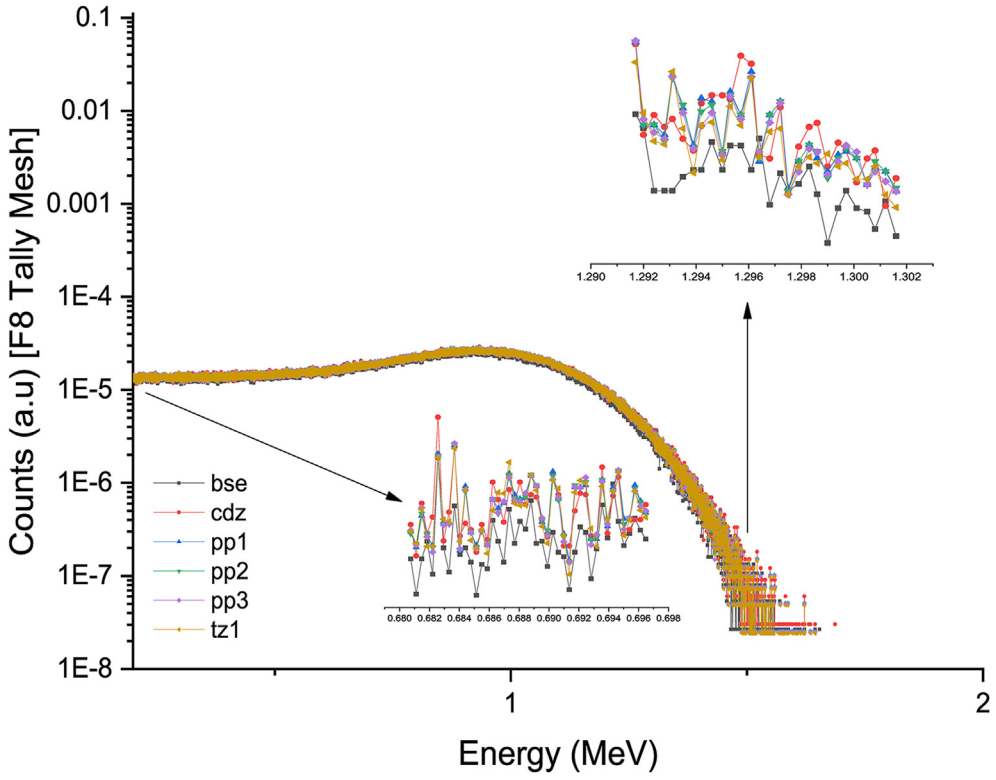

Fig. 4. Comparison of pulse/height distributions for modelled scintillation crystals.

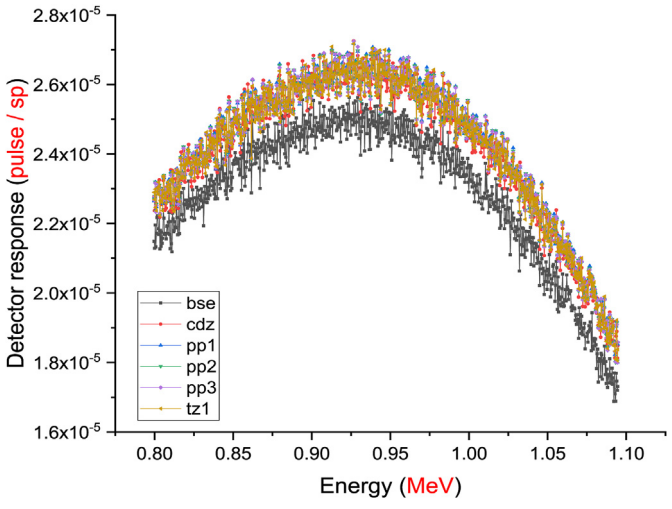

Fig. 5. Comparison of detector responses for modelled scintillation crystals.

Table 3
Deposited energy values obtained from F6 Tally Mesh in modelled scintillation crystals.

Scintillator type	Deposited energy (MeV/g)
bse	7.13144E-06
cdz	7.54138E-06
pp1	7.56628E-06
pp2	7.56114E-06
pp3	7.55580E-06
tz1	7.54011E-06

scintillation crystal is the consequence of the interaction of a gamma ray with the crystal's atomic structure. In other words, a higher percentage of collision between the crystal material and the gamma-ray population may cause an increase in the number of produced optical photons to be produced to be at higher values. As shown in the figure, the proportionate tendency to collide was determined for each population at the maximum rate in the pp1 crystal and at the lowest rate in the bse detector. This situation may

Table 2
Obtained results of plastic scintillation detectors from the MCNPX OUTPUT file.

Results	Scintillator type					
	bse	cdz	pp1	pp2	pp3	tz1
Tracks entering	9683610	8534330	10134786	10134707	10306306	10667783
Population	9795277	8628847	10244709	10244983	10418873	10782904
Collisions	3106356	2930153	3488417	3485735	3542160	3655261
Collision weight per history	8.29E+02	8.87E+02	8.89E+02	8.88E+02	8.88E+02	8.85E+02
Number weighted energy	1.11E+04	1.11E+04	1.11E+04	1.11E+04	1.11E+04	1.11E+04
Flux weighted energy	1.11E+04	1.11E+04	1.11E+04	1.11E+04	1.11E+04	1.11E+04
Average track mfp (cm)	1.54E+05	1.44E+05	1.43E+05	1.43E+05	1.43E+05	1.44E+05
Collision per population (%)	317.127	339.576	340.509	340.238	339.975	338.986

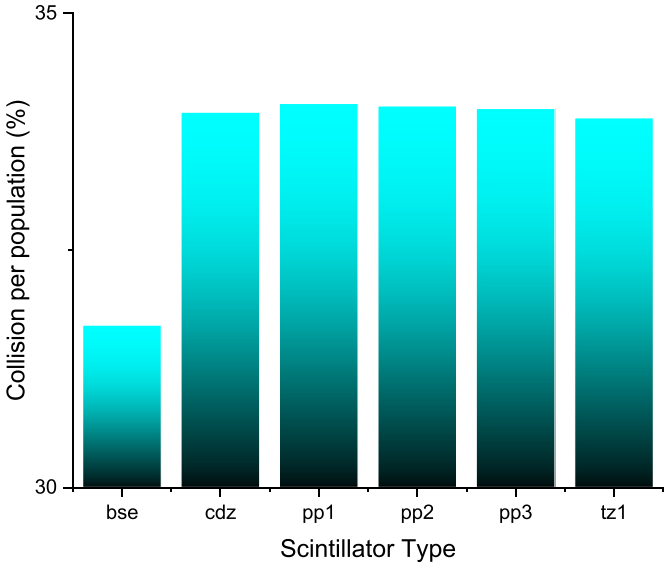

Fig. 6. Variation of collision per population for modelled scintillation crystals.

be seen as a critical factor ensuring the consistency of earlier results. The reason for this is because the low collision rate in the bse detector per population resulted in a low number of signals, which resulted in the bse spectra obtaining an average count value. On the other hand, quantity of collision per population for pp1 was observed as maximum. Meanwhile, the mean free path can be defined as the mean distance travelled by a gamma-ray before undergoing the first interaction. While the low mfp value for shielding materials is attributed to the superior absorption properties, the low value for scintillation crystals indicates that the individual gamma rays will interact sequentially at shorter distances, resulting in relatively faster signal generation at shorter distances. That is, the shorter the distance necessary for the second interaction (lower mfp value) after the signal established by the gamma ray's initial contact, the more likely the second signal will be produced in a shorter period and more rapidly. Fig. 7 depicts the variation of average track mean free path (cm) for modelled scintillation crystals. As shown in the figure, the minimum mfp values belongs to pp1, while the maximum for bse. Additionally, the average difference between the pp1 and bse is almost 1 cm, indicating that those two scintillation crystals have a nearly 1 cm difference in terms of having two adjacent gamma-ray and crystal interactions in the detector. In the final phase of the study, the energy deposition amounts (MeV/g) occurring in the scintillation area shown in Fig. 2 for six different plastic scintillation crystals were calculated separately by using the F6 Tally Mesh properties of MCNPX code. In MCNPX code, F6 tally mesh provides the energy deposition (MeV/g). As with any radiation detector, a scintillator is an absorbent material that also could convert a part of the energy deposited by ionizing radiation to light [43]. Fig. 8 depicts the variation of deposited energy amounts (MeV/g) for investigated plastic scintillation crystals. Clearly, the crystal with the greatest quantity of deposited energy is the pp1 crystal. By comparison, bse has the lowest deposited energy levels. As once scintillator material is bse, incoming photons are very likely to pass through with a low number of collisions. Each gamma-ray-crystal interaction in the scintillation crystal results in a reduction in the energy of the gamma-ray. The increase in collisions per population, as previously noted for the pp1 crystal, also resulted in an increase in the quantity of energy transmitted to the environment because of these collisions. Consequently, the quantity of energy deposited at the maximum as a result of the maximum collision was observed.

4. Conclusion

In recent years, there has been an increasing interest in the use of plastic scintillation detectors (PSD) for the detection and measurement of ionizing radiation. Plastic scintillation detectors are manufactured in a wide variety of different geometries and sizes, such as thin sheets, rods, rings and large rectangular blocks. Larger volume detectors are used to measure gamma radiation. Plastic itself is not useful as a scintillator due to its very low fluorescence efficiency. To make an efficient scintillator, in addition to polystyrene, primary flour doped about 1% by weight and a spectrum shifter doped about 0.01% by weight are usually used. The doped compounds are determined according to their photophysical properties. The deposition of energy from ionizing radiation in the PSD material is important for fluorescence to occur. The need for nuclear measurement methods and gamma spectroscopy methods

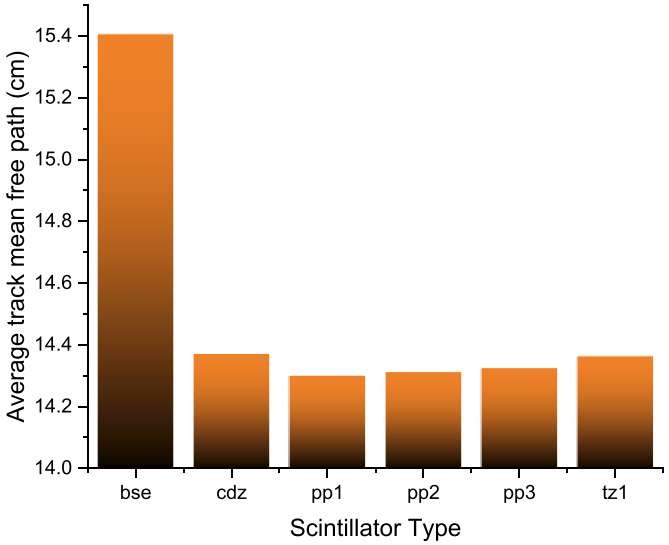

Fig. 7. Variation of average track mean free path (cm) for modelled scintillation crystals.

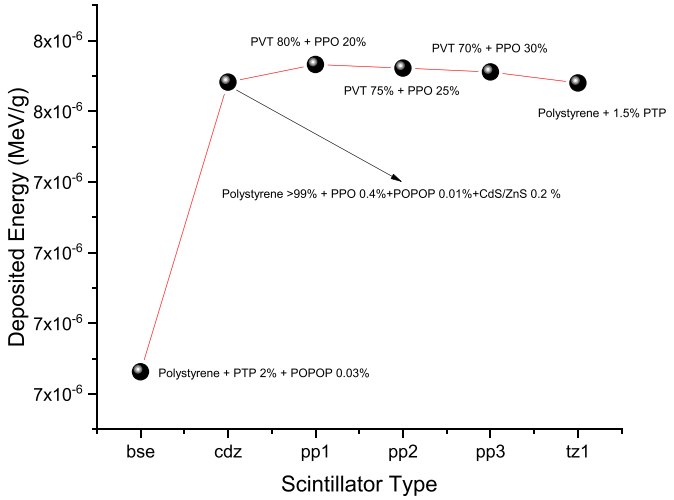

Fig. 8. Variation of deposited energy amounts (MeV/g) for investigated plastic scintillation crystals.

is increasing day by day in line with scientific and industrial expectations. One of the equipment used for gamma-ray spectroscopy is plastic scintillation detectors. Plastic scintillators are widely used in a number of radiation measurement applications, and their use in nuclear applications such as gamma-ray detection and measurement raise serious concerns. It is vital to optimize the plastic scintillator crystal for effective and successful gamma-ray detection. The objective of this extensive study is to determine how to evaluate the scintillator crystal's effect on the whole detection process. MCNPX (version 2.6.0) is utilized in our laboratory to construct a physical plastic scintillation detector. Although the compositions of six scintillation crystals are similar, the results clearly demonstrate that the crystal formed of PVT 80% + PPO 20% has better counting and detecting properties when compared to the other crystals tested. Additionally, it was discovered that the maximum deposited energy amount corresponds to a PVT 80% + PPO 20% crystal, because of the highest collision number in the crystal volume. Despite the similar chemical structures of plastic detector crystals, this study discovered that performing advanced Monte Carlo simulations on the detected discrepancies within the structures can aid in the development of the most effective spectroscopy procedures by ensuring maximum efficiency prior to and during use. Moreover, it can be concluded that the total cross-section of the WLS and LY in a SCINT comprising the light-collecting matters, which must be optically connected to the PMT photocathodes can be used and the detector can be made more compact and significantly more cost-efficient.

Funding

Princess Nourah bint Abdulrahman University Researchers Supporting Project Number (PNURSP2022R149).

Data availability statement

The data presented in this study are available on request from the corresponding author.

Declaration of competing interest

The authors declare that they have no known competing financial interests or personal relationships that could have appeared to influence the work reported in this paper.

The authors declare no conflict of interest.

Acknowledgements

Authors express their sincere gratitude to Princess Nourah bint Abdulrahman University Researchers Supporting Project Number (PNURSP2022R149), Princess Nourah bint Abdulrahman University, Riyadh, Saudi Arabia.

References

[1] Matthieu Hamel, Plastic scintillators chemistry and applications. https://doi.org/10.1007/978-3-030-73488-6.
[2] Branislav Stríbrnský, et al., Energy calibration of plastic scintillator detector, AIP Conf. Proc. 2131 (2019), 020044, https://doi.org/10.1063/1.5119497.
[3] M.G. Schorr, F.L. Torney, Phys. Rev. 80 (3) (1950) 474.
[4] Sujung Min, et al., Optimization of plastic scintillator for detection of gamma-rays: simulation and experimental study, Chemosensors 9 (2021) 239, https://doi.org/10.3390/chemosensors9090239, 2021.
[5] S. Min, H. Kang, et al., Integrated and portable probe based on functional plastic scintillator for detection of radioactive cesium, Appl. Sci. 11 (2021) 5210.
[6] M. Hamel, et al., Plastic Scintillators Modifications for a Selective Radiation Detection, 2019.
[7] H.R. Kang, et al., Preliminary studies of perovskite-loaded plastic scintillator prototypes for radioactive strontium detection, Chemosensors 9 (2021) 53.
[8] J.M. Park, et al., Scintillation properties of quantum-dot doped styrene based plastic scintillators, J. Lumin. 146 (2014) 157–161.
[9] J.S. Nam, et al., Performance evaluation of a plastic scintillator for making a in-situ beta detector, New Phy. Sae Mulli 67 (2017) 1080–1085.
[10] Cheol HoLee, et al., Characteristics of plastic scintillators fabricated by a polymerization reaction, Nucl. Eng. Technol. 49 (Issue 3) (April 2017) 592–597.
[11] Yuki Araya, et al., Enhanced detection efficiency of plastic scintillators upon incorporation of zirconia nanoparticles, Sens. Mater. 27 (No. 3) (2015) 255–261.
[12] C. Kim, et al., Simulation Study of a Plastic Scintillator for an Electrical Personal Dosimeter, IEEE, 2013, 978-1-4799-0534-8/13/$31.00 ©.
[13] Zafar Yasin, Florin Negoita, Sana Tabbassum, et al., Monte Carlo simulations and measurements for efficiency determination of lead shielded plastic scintillator detectors, https://doi.org/10.1063/1.5017442.
[14] Abdullah Mohammad Shehada, et al., MCNP simulations for silver-plastic scintillator detector for mono-energy neutrons 2.5 and 14 MeV. ISSN 1547-4771, Phys. Part. Nuclei Lett. 18 (7) (2021) 786–790.
[15] Rogers, T and et al, Synthesis of Luminescent Nanoparticle Embedded Polymer Nanocomposites for Scintillation Applications, DOI: 10.1557/opl.2011.123.
[16] Patrick L. Feng, et al., Distance dependent quenching and gamma-ray spectroscopy in tin-loaded polystyrene scintillators, IEEE Transact. Nucl. Sci. 63 (1) (FEBRUARY 2016).
[17] Henok A. Yemam et al. Highly Soluble P-Terphenyl and Fluorene Derivatives as Efficient Dopants in Plastic Scintillators for Sensitive Nuclear Material Detection. DOI: 10.1002/chem.201700877.
[18] A. Lim, et al., Plastic scintillators with efficient light output and pulse shape discrimination produced via photoinitiated polymerization, J. Appl. Polym. Sci. (2018), https://doi.org/10.1002/app.47381.
[19] Hart. Alexander, et al., Lead-doped scintillator dosimeters for detection of ultrahigh dose-rate x-rays, Phys. Med. Biol. 67 (2022), 105007.
[20] Min. S, et al., Integrated and portable probe based on functional plastic scintillator for detection of radioactive cesium, Appl. Sci. 11 (2021) 5210, https://doi.org/10.3390/app11115210.
[21] V. Villemot, et al., From sintering to particle discrimination: new opportunities in metal–organic frameworks scintillators, Adv. Photonics Res. 3 (2022), 2100259.
[22] Alan Proctor, Deconvolving plastic scintillator gamma-ray spectra using particle Swarm optimization, in: IEEE Nuclear Science Symposium and Medical Imaging Conference, 2020, https://doi.org/10.1109/NSS/MIC42677.2020.9507902. NSS/MIC)978-1-7281-7693-2/20/$31.00©2020IEEE.
[23] F. Horst, et al., A.multi-detector experimental setup for the study of space radiation shielding materials: measurement of secondary radiation behind thick shielding and assessment of its radiobiological effect, EPJ Web of Conferences 261 (2022), 03002, https://doi.org/10.1051/epjconf/202226103002, 2022.
[24] Koutaro Yamasoto, Masahiro Tsutsumi, Tetsuya Oishi, Michio Yoshizawa, Makoto Yoshida, CsI(Tl)/plastic phoswich detector enhanced in low-energy gamma-ray detection, Nucl. Instruments Methods Phys. Res. Sec. A: Accelerators, Spectrometers, Detect. Assoc. Equip. 550 (2005) 609–615, https://doi.org/10.1016/j.nima.2005.05.054.
[25] Lino Miramonti, A plastic scintillator detector for beta particles, Radiat. Meas. 35 (2002) 347–354, https://doi.org/10.1016/S1350-4487(02)00051-3.
[26] R. Shweikani, G. Raja, A.A. Sawaf, The possibility of using plastic detectors CR-39 as UV dosimeters, Radiat. Meas. 35 (2002) 281–285, https://doi.org/10.1016/S1350-4487(02)00055-0.
[27] V. Andreev, J. Cvach, M. Danilov, E. Devitsin, V. Dodonov, G. Eigen, E. Garutti, Yu. Gilitzky, M. Groll, R.-D. Heuer, M. Janata, I. Kacl, V. Korbel, V. Kozlov, H. Meyer, V. Morgunov, S. Němeček, R. Pöschl, I. Polák, A. Raspereza, S. Reiche, V. Rusinov, F. Sefkow, P. Smirnov, A. Terkulov, Š. Valkár, J. Weichert, J. Zálešák, A high-granularity plastic scintillator tile hadronic calorimeter with APD readout for a linear collider detector, Nucl. Instruments Methods Phys. Res. Sec. A: Accelerators, Spectrometers, Detect. Assoc. Equip. 564 (2006) 144–154, https://doi.org/10.1016/j.nima.2006.04.044.
[28] A.A.R. Da Silva, E.M. Yoshimura, Track analysis system for application in alpha particle detection with plastic detectors, Radiat. Meas. 39 (2005) 621–625, https://doi.org/10.1016/j.radmeas.2004.06.018.
[29] K. Kawagoe, Y. Sugimoto, A. Takeuchi, T. Asakawa, J.P. Done, Y. Fujii, K. Furukawa, F. Kajino, T. Kamon, N. Kanaya, J. Kanzaki, S. Kim, A. Nakagawa, M. Nozaki, R. Oishi, T. Ota, H. Takeda, T. Takeshita, S. Uozumi, Performance of preshower and shower-maximum detectors with a lead/plastic-scintillator calorimeter, Nucl. Instruments Methods Phys. Res. Sec. A: Accelerators, Spectrometers, Detect. Assoc. Equip. 487 (2002) 275–290, https://doi.org/10.1016/S0168-9002(01)00890-7.
[30] B.M. Moharram, Lamaze George, M. Elfiki, N. Khalil, Neutron-based analysis of fission rates and ultra-trace concentrations of 235U using gamma spectrometry and CR-39 (plastic track detector), Radiat. Meas. 35 (2002) 113–117, https://doi.org/10.1016/S1350-4487(01)00277-3.
[31] M. Fromm, Light MeV-ions etching studies in a plastic track detector, Radiat. Meas. 40 (2005) 160–169, https://doi.org/10.1016/j.radmeas.2005.04.028.
[32] A. Artikov, J. Budagov, I. Chirikov-Zorin, D. Chokheli, M. Lyablin, G. Bellettini, A. Menzione, S. Tokar, N. Giokaris, A. Manousakis-Katsikakis, Properties of the Ukraine polystyrene-based plastic scintillator UPS 923A, Nucl. Instruments Methods Phys. Res. Sec. A: Accelerators, Spectrometers, Detect. Assoc. Equip.

555 (2005) 125–131, https://doi.org/10.1016/j.nima.2005.09.021.
[33] RSICC Computer Code Collection, MCNPX user's manual version 2.4.0. MonteCarlo N-Particle Transport Code System for Multiple and High Energy Applications, 2002.
[34] H.O. Tekin, Ghada ALMisned, Shams A.M. Issa, Hesham M.H. Zakaly, A rapid and direct method for half value layer calculations for nuclear safety studies using MCNPX Monte Carlo code, Nucl. Eng. Technol. (2022), https://doi.org/10.1016/j.net.2022.03.037. Available Online 29 March 2022.
[35] H.O. Tekin, Fatema T. Ali, Ghada Almisned, Gulfem Susoy, Shams A.M. Issa, Antoaneta Ene, Wiam Elshami, M. Hesham, H. Zakaly, Multiple assessments on the gamma-ray protection properties of niobium-doped borotellurite glasses: a wide range investigation using Monte Carlo simulations, Sci. Technol. Nucl. Installations (2022), 5890896, https://doi.org/10.1155/2022/5890896.
[36] Aylin M. Deliormanlı, Mertcan Ensoylu, A. Shams, M. Issa, Y.S. Rammah, Ghada ALMisned, H.O. Tekin, A thorough examination of gadolinium (III)-containing silicate bioactive glasses: synthesis, physical, mechanical, elastic and radiation attenuation properties, Appl. Phys. A 128 (2022) 266, https://doi.org/10.1007/s00339-022-05408-0.
[37] W. Elshami, H.O. Tekin, Shams A.M. Issa, Mohamed M. Abuzaid, Hesham M. Zakaly, Bashar Issa, Antoaneta Ene, Impact of eye and breast shielding on organ doses during the cervical spine radiography: design and validation of MIRD computational phantom, Front. Public Health (2021), https://doi.org/10.3389/fpubh.2021.751577. Received: 01 Aug 2021; Accepted: 27 Sep. 2021.
[38] Ghada ALMisned, M. Hesham, H. Zakaly, Shams A.M. Issa, Antoaneta Ene, Gokhan Kilic, Omemh Bawazeer, Albandari Almatar, Dalal Shamsi, Elaf Rabaa, Zuhal Sideig, H.O. Tekin, Gamma-ray protection properties of bismuth-silicate glasses against some diagnostic nuclear medicine radioisotopes: a comprehensive study, Materials 14 (2021) 6668, https://doi.org/10.3390/ma14216668.
[39] Ghada ALMisned, Wiam Elshami, A. Shams, M. Issa, G. Susoy, H.M.H. Zakaly, M. Algethami, Y.S. Rammah, A. Ene, S.A. Al-Ghamdi, A.A. Ibraheem, H.O. Tekin, Enhancement of gamma-ray shielding properties in cobalt-doped heavy metal borate glasses: the role of lanthanum oxide reinforcement, Materials 14 (2021) 7703, https://doi.org/10.3390/ma14247703.
[40] H.O. Tekin, Ghada ALMisned, Shams A.M. Issa, Emel Serdaroglu Kasikci, Mahreen Arooj, Anoaneta Ene, M.S. Al-Buriahi, Muhsin Konuk, M. Hesham, H. Zakaly, Molecular polar surface area, total solvent accessible surface area (SASA), heat of formation and gamma ray attenuation properties of some flavonoids, Front. Phys. 10 (2022), 838725, https://doi.org/10.3389/fphy.2022.838725.
[41] Kelly D. Rakes, Master Thesis, Evaluating the Response of Polyvinyl Toluene Scintillators Used in Portal Detectors, Air Force Institute of Technology, Air University, 2008. AFIT/GNE/ENP/08-M04.
[42] [a] Avneet Sood, R.A. Forster, Bryce J. Adams, Morgan C. White, Verification of the pulse height tally in MCNP 5.Nuclear Instruments and Methods in Physics Research Section B: Beam Interactions with Materials and Atoms, 213, 2004, pp. 167–171, https://doi.org/10.1016/S0168-583X(03)01598-2;
[b] Jing Sun, Robin P. Gardner, Optimization of the steady neutron source technique for absorption cross section measurement by using an 124Sb–Be neutron source, Nucl. Instruments Methods Phys. Res. Sect. B: Beam Interact. Mater. Atoms 213 (2004) 22–28, https://doi.org/10.1016/S0168-583X(03)01527-1.
[43] P. Lecoq, Scintillation detectors for charged particles and photons, in: C. Fabjan, H. Schopper (Eds.), Particle Physics Reference Library, Springer, Cham, 2020, https://doi.org/10.1007/978-3-030-35318-6_3.